scientific reports

Check for updates

OPEN

Modified RECIST submodels and ordinal regression model predict neoadjuvant chemoimmunotherapy response in locally advanced gastric cancer

Shu Chen, Shenghong Wei, Zaisheng Ye, Cheng Wei, Sheng Liu, Yi Wang, Yi Zeng, Jinhu Chen, Xiaopeng Wang, Jianping Jiang, Xiaoling Chen & Luchuan Chen✉

This study evaluated predictive models integrating Computed Tomography(CT) and ultrasound(US) to assess neoadjuvant therapy response in locally advanced gastric cancer (LAGC). A prospective multicenter trial (*n* = 75) developed five RECIST 1.1-derived submodels (RECIST_Expansion, UC_RECIST, CT_RECIST, V-RECIST, U-RECIST) and an ordinal regression-based nomogram, using pathological tumor regression grade (TRG) as the reference standard. The geometric approximation model V-RECIST exhibited superior diagnostic performance for TRG 0–2 vs. 3 discrimination (area under the curve [AUC] = 0.951, sensitivity 96.8%/specificity 80.1%) and TRG 0–1 vs. 2–3 classification (AUC = 0.868, sensitivity 85.7%/specificity 80.0%), validated by calibration curves and decision curve analysis. The US-only U-RECIST demonstrated good diagnostic accuracy (AUC = 0.906/0.811), suitable for preliminary assessment due to its safety and cost-effectiveness. The remaining models—RECIST_ Expansion (lymph node evaluation only), UC_RECIST (CT-US combined protocol with gastric lesions as measurable targets), and CT_RECIST (CT-only for no-US settings)—also showed satisfactory accuracy. The ordinal regression model achieved slightly higher AUC values (0.952/0.870) and cross-validation accuracy (0.73) compared to modified RECIST models. These findings highlight the clinical utility of revised RECIST 1.1 models across diverse scenarios, with V-RECIST demonstrating the highest performance, U-RECIST offering radiation-free assessment and cost-effectiveness, and the ordinal model enhancing visualization while preserving diagnostic superiority.

Keywords Local advanced gastric cancer (LAGC), Neo-adjuvant therapy, Chemoimmunotherapy, RECIST, Color doppler ultrasound; nomogram model

Gastric cancer (GC) remains a major global health burden, ranking sixth in incidence and third in mortality[1]. In 2020, 1.089 million new cases and 769,000 deaths were reported globally[2] with China contributing 43.94% of global incidence (478,508 cases)[3]. GC prognosis is stage-dependent, with 5-year survival rates between 20% and 40% globally. For locally advanced gastric cancer (LAGC), this drops below 30%, necessitating surgery-centered comprehensive treatment[4]. Neoadjuvant chemotherapy (NAC) is now the global standard for LAGC, supported by trials like Germany's FLOT4-AIO[5] and Asia's RESOLVE[6]. The Orient-16 trial[7] established PD-1 inhibitor-based immunotherapy combined with chemotherapy as a first-line option for unresectable locally advanced, recurrent, or metastatic gastric/gastroesophageal junction (GEJ) adenocarcinoma.

However, standardized methods for evaluating neoadjuvant therapy efficacy remain limited. The international community primarily uses WHO criteria[8] and RECIST 1.1[9]. WHO criteria assess response via the product of longest tumor diameter and its perpendicular counterpart, while RECIST 1.1 defines target lesions and evaluates changes in total diameters from baseline[10]. Because the stomach is non-solid, primary gastric lesions are classified as non-measurable under RECIST, with lymph nodes ≥ 1.5 cm in short axis considered measurable[11]. This limitation hinders preoperative assessments, delaying precision medicine and optimal surgical timing.

Department of Gastric Surgery, Clinical Oncology School of Fujian Medical University, Fujian Cancer Hospital，NHC Key Laboratory of Cancer Metabolism, No 420 Fuma Road, Jin'an District, Fuzhou 350000, Fujian Province, China. ✉email: sheeook@163.com

To address this, researchers proposed modified criteria (e.g., irRECIST[12] and imRECIST[13] and functional imaging standards (e.g., EORTC[14] and PERCIST 1.0[15]). Techniques like contrast-enhanced ultrasound(US), dual-source Computed Tomography(CT) iodine uptake measurement, MRI-derived ADC values, and AI-integrated imaging with multi-omics strategies show high sensitivity and specificity. However, no universally accepted method exists due to applicability challenges, despite their accuracy.

In parallel with a prospective study on NAC combined with immunotherapy for LAGC, our team evaluated high-resolution CT and color Doppler ultrasound against postoperative TRG using the CAP system[16]. The goal was to assess models derived from routine methods in evaluating therapeutic outcomes after neoadjuvant treatment, providing a clinically relevant tool for efficacy evaluation.Materials and Methods.

Methods

Data collection

This study compiled multi-center data from the investigation of "Tislelizumab combined with Apatinib and chemotherapy as neoadjuvant treatment for Borrmann IV type, large Borrmann III type, and Bulky N LAGC. "Data were collected from five Fujian-based hospitals: Fujian Cancer Hospital, Sanming First Hospital, Sanming Second Hospital, Putian University Affiliated Hospital, and Xiapu County Hospital.

Inclusion criteria

- ECOG performance status of 0–1;
- Age 18–75 years;
- Histologically confirmed AJCC 8th edition LAGC, with tumors > 5 cm in basal diameter categorized as Borrmann III, Borrmann IV, or Bulky N (enlarged lymph nodes > 3 cm around specific gastric regions or more than two adjacent lymph nodes > 1.5 cm);
- Preoperative endoscopy confirming no peritoneal dissemination and negative cytology;
- No prior surgery, radiotherapy, chemotherapy, or immunotherapy.

Exclusion criteria

- History of other malignant tumors;
- Acute oncological emergencies (bleeding, obstruction, perforation);
- Known HER2 positivity;
- Allergy to study drugs;
- Conditions interfering with trial outcomes;
- Mucinous adenocarcinoma and lymphoepithelioma-like carcinoma, excluded due to reduced TRG grading accuracy in pathology assessments.
- The study was approved by the Ethics Committees of all participating institutions.

Treatment regimen(each 21-day cycle):

- Tislelizumab (TSZ): 200 mg IV on Day 1.
- Apatinib (APA): 250 mg/day orally (Days 1–21).
- Oxaliplatin (OXA): 130 mg/m² IV on Day 1.
- S-1: Oral dosing based on BSA (Days 1–14):
- < 1.25 m²: 40 mg bid.
- 1.25–1.50 m²: 50 mg bid.
- ≥ 1.50 m²: 60 mg bid.

Four cycles were administered, with APA omitted in the final cycle, followed by gastrectomy with D2 lymphadenectomy and R0 resection. Imaging assessment was performed per modified RECIST 1.1.

Imaging protocols

Imaging modalities included CT scans with a slice thickness of ≤ 5 mm, using oral negative contrast for stomach expansion, followed by low-dose preparation and iodinated contrast enhancement. Color Doppler ultrasonography involved the patient consuming 400-500 ml of a gastrointestinal ultrasound contrast agent in a semi-solid state prepared with hot water 5 min before the exam. Scanning in various positions assessed lesion location, size, local gastric wall structure, depth of infiltration, gastric motility, and the presence of lymphadenopathy or metastasis to adjacent organs.

- CT: ≤5 mm slice thickness, oral negative contrast for stomach expansion, low-dose prep, and iodinated contrast.
- Color Doppler US: Patients ingested 400–500 mL of semi-solid ultrasound contrast (prepared with hot water 5 min pre-exam).
- Assessment Parameters: Lesion location, size, gastric wall structure, infiltration depth, motility, lymphadenopathy, and organ metastasis.
- Image Interpretation Measures.
- Standardized SOPs: Unified reading guidelines and SOPs ensured consistent evaluation.
- Blinded Review: Readers had no access to patient identifiers or clinical data.
- CAD Systems: Reduced subjectivity via computer-aided diagnosis (CAD).
- Training & Certification: Readers completed skill-specific training programs.

- Inter-Rater Reliability: Kappa value testing monitored agreement rates.
- Dual Review: CT: 2 radiologists reviewed independently; discrepancies resolved by consensus; US: 2 sonographers reviewed independently; discrepancies resolved by consensus.
- Re-Reading: Critical/controversial cases underwent multi-reader/multi-examiner re-evaluation for CT/US. Pathological Assessment.

Pathological response assessment (TRG System)

TRG (American Society of Clinical Oncology): This study's pathological review provided detailed definitions for the percentage of residual cancer cells in each grade, as follows:

1. TRG 0 = No viable cancer cells (complete response, 0% residual cells).
2. TRG 1 = Isolated or small clusters of residual cells (moderate response, < 10% residual cells).
3. TRG 2 = Residual tumor with fibrosis (minimal response, 10–90% residual cells).
4. TRG 3 = Minimal or no tumor regression, abundant residual cancer cells• (poor response, > 90% residual cells).

Efficacy evaluation criteria design

The first category of evaluation criteria adopted the classical Response Evaluation Criteria in Solid Tumors (RECIST, version 1.1)[17] Models were established using ultrasound-measured gastric tumor diameters. To address diverse clinical scenarios and imaging limitations, five distinct evaluation methods were designed and validated against pathological tumor regression grades (TRG) via Receiver Operating Characteristic(ROC) curves, calibration curves, and Decision Curve Analysis (DCA) curves. Standard RECIST v1.1[18,19] defines measurable lymph nodes as those with a short-axis diameter > 1.5 cm, which remains the mainstream standard. However, diagnostic studies have proposed lower thresholds (0.5–0.7 cm), requiring integration of morphology, long-to-short axis ratio, enhancement pattern, and margin characteristics. Radiomics techniques, which extract thousands of features (e.g., textural, wavelet) for machine learning[20–24].

Through prospective internal validation at our center using postoperative pathology confirmation, we demonstrated that a lymph node short-axis threshold of ≥ 0.7 cm achieved 62% sensitivity and 91% specificity. Therefore, this study adopted ≥ 0.7 cm as the threshold. Final lymph node positivity assessments required comprehensive evaluation combining morphology, enhancement patterns, and other features. We recommend that medical centers carefully consider local technology and validation data before adjusting the > 1.5 cm gold standard.

Abbreviations include Sum of short axes of lymph nodes measured by CT = CT Lymph Node Diameter Sum; Maximum short axis of lymph nodes measured by CT = CT Lymph Node Diameter; Maximum thickness of gastric lesion measured by CT = CT Gastric Lesion Thickness; Maximum basal width of gastric lesion measured by ultrasound = US Gastric Lesion Base Width; Maximum thickness of gastric lesion measured by ultrasound = US Gastric Lesion Thickness. Pre-tx/Post-tx (before/after treatment).

RECIST_Expansion group: This cohort evaluated the predictive accuracy of RECIST 1.1 in estimating TRG. Following standard RECIST 1.1 methodology, gastric primary lesions were classified as non-measurable targets, with treatment response assessed solely via CT-measured changes in the sum of lymph node short-axis diameters. However, clinically, lymph nodes > 1.5 cm are rarely observed. According to recent Literature and our prospective validation, we recommend a reduced threshold of 0.7 cm for the short-axis diameter of lymph nodes.

Evaluation formula: Shrinkage rate =

$$\frac{(\text{Pre}-\text{tx})\text{CT Lymph Node Diameter Sum} - (\text{Post}-\text{tx})\text{CT Lymph Node Diameter Sum}}{(\text{Pre}-\text{tx})\ \text{CT Lymph Node Diameter Sum}}$$

UC_RECIST Group(Ultrasound-Modified RECIST Group): While RECIST 1.1 defines measurable lesions (> 10 mm longest diameter), gastric lesions are categorized as non-measurable due to their hollow viscus anatomy. This cohort explored reclassifying gastric lesions as measurable targets using ultrasound-measured basal width as the longest diameter. Treatment response was evaluated by combining this parameter with CT-assessed lymph node regression.

Evaluation formula: Shrinkage rate=

$$\frac{\text{Pre}-\text{tx}(\text{CT Lymph Node Diameter Sum} + \text{US Gastric Lesion Base Width}) - \text{Post}-\text{tx}(\text{CT Lymph Node Diameter Sum} + \text{US Gastric Lesion Base Width})}{\text{Pre}-\text{tx}(\text{CT Lymph Node Diameter Sum} + \text{US Gastric Lesion Base Width})}$$

CT_RECIST Group(CT-Only RECIST Group): Not all centers can use ultrasound for gastric tumor assessment; CT is more widely accessible. This cohort established CT-exclusive criteria to validate their accuracy. Due to CT's limitations in measuring gastric lesion basal width, treatment response was assessed via CT-measured gastric lesion thickness changes and lymph node regression.

Evaluation formula: Shrinkage rate=

$$\frac{\text{Pre}-\text{tx}(\text{CT Lymph Node Diameter} + \text{CT Gastric Lesion Thickness} - \text{Post}-\text{tx}(\text{CT Lymph Node Diameter} + \text{CT Gastric Lesion Thickness})}{\text{Pre}-\text{tx}(\text{CT Lymph Node Diameter} + \text{CT Gastric Lesion Thickness})}$$

U_RECIST Group(Ultrasound-Only RECIST Group): As a radiation-free, cost-effective modality, ultrasonography enables more frequent monitoring than CT during treatment cycles. This facilitates earlier

detection of disease progression, enhancing precision oncology strategies. This cohort evaluated ultrasound alone as a safer, clinically accurate alternative for treatment response assessment.

Evaluation formula: Shrinkage rate=

$$\frac{(\text{Pre}-\text{tx US Gastric Lesion Base Width}/2)^2 \times (\text{Pre}-\text{tx US Gastric Lesion Thickness}) - (\text{Post}-\text{tx US Gastric Lesion Base Width}/2)^2 \times (\text{Post}-\text{tx US Gastric Lesion Thickness})}{(\text{Pre}-\text{tx US Gastric Lesion Base Width}/2)^2 \times (\text{Pre}-\text{txUS Gastric Lesion Thickness})}$$

V_RECIST Group(Volumetric RECIST Group): To combine strengths of CT and ultrasound, this cohort used an approximate volume formula, integrating: CT-measured maximum lymph node short-axis diameter, CT-measured gastric lesion thickness, and Ultrasound-measured gastric lesion basal width.Pre- and post-treatment changes in lymph node and gastric tumor volumes were modeled to optimize monitoring accuracy.

Evaluation formula: Shrinkage rate=

$$\frac{\text{the Shrinkage rate of U}-\text{RECIST Group}}{2} + \frac{\text{Pre}-\text{tx CT Lymph Node Diameter}^2 - \text{Post}-\text{tx CT Lymph Node Diameter}^2}{2 \times \text{Pre}-\text{tx CT Lymph Node Diameter}^2}$$

Category 2 efficacy evaluation

Patients were stratified into three groups based on TRG classification: MPR Group (TRG 0–1), Partial Response Group (TRG 2), and No Response Group (TRG 3). A regression model and nomogram were developed using ordinal logistic regression for univariate and multivariate analyses to identify key predictors,. Model performance was assessed via ROC curves, calibration curves, DCA curves, and ten-fold cross-validation.

Statistical analyses

Statistical analyses were carried out with SPSS 20.0[25], and categorical variables were summarized as counts (%). Agreement between TRG and imaging assessments was evaluated via ROC curves, determining optimal cut-off values, sensitivity, specificity, and P-values ($P<0.05$ indicated significance). Calibration curves and DCA were generated using R 4.4.0[26], alongside ordinal logistic regression (univariate and multivariate) and nomogram construction. Model performance was validated through ROC curves, calibration curves, DCA curves, and ten-fold cross-validation.

Results

Clinical data statistics

This study utilized data from 75 patients enrolled in phase II and some phase III studies on "Tislelizumab combined with Apatinib and chemotherapy as neoadjuvant treatment for Borrmann IV type, large Borrmann III type, and Bulky N LAGC". Among them, 56 (74.6%) were male, and 40 (53.3%) presented with poorly differentiated gastric tumors. By GC type, 47 (63.7%) had Large Borrmann III Type, and 26 (34.6%) achieved TRG grade 2. Detailed patient characteristics are summarized in Table 1.

Establishment of model category 1 - Efficacy evaluation model based on tumor diameter according to RECIST (Version 1.1)

1) Model Development and Evaluation

Efficacy groups were defined by TRG grades: Grades 0–2 (effective), Grade 3 (ineffective). ROC analysis showed the V_RECIST group had the highest area under the receiver operating characteristic curve [AUC] (0.951) at the optimal cutoff, indicating superior predictive accuracy. The UC_RECIST, CT_RECIST, and U_RECIST groups achieved AUCs of 0.909, 0.933, and 0.906, respectively, all non-inferior to RECIST_Expansion (AUC = 0.915) (Table 2; Fig. 1a). All models demonstrated good sensitivity and specificity.Calibration curves confirmed strong agreement between predicted and observed outcomes (Mean Absolute Error (MAE), Mean Squared Error (MSE), and 0.9 Quantile of absolute error(Q90 (AE))(Fig. 1b; Table 3). DCA curves validated clinical utility, with V_RECIST providing net benefits above ALL/None thresholds. Other groups also showed satisfactory performance (Fig. 1c).

2) Evaluation by MPR

The patients were reclassified into TRG 0–1 (MPR) and TRG 2–3 (Non-MPR) groups. ROC analysis showed V_RECIST achieved the highest AUC (0.868) at the optimal cutoff, outperforming UC_RECIST (0.804), CT_RECIST (0.842), U_RECIST (0.811), and RECIST_Expansion (0.778) (Table 2; Fig. 1d). All models demonstrated acceptable sensitivity and specificity.Calibration metrics (MAE, MSE, 0.9 Quantile of Absolute Error) confirmed strong alignment between predicted and actual outcomes (Table 3). DCA curves validated clinical utility, with V_RECIST consistently yielding net benefits above "ALL" and "None" thresholds. Other models also showed satisfactory performance for diverse scenarios (Fig. 1e, f).

Establishment of the second category prediction model: ordered logistic regression and nomogram model

To develop the second category prediction model, patients were stratified into three TRG groups: MPR (TRG 0–1), Partial Response (TRG 2), and No Response (TRG 3). Variables included imaging data and pre-treatment biomarkers: CPS, differentiation, neutrophil-to-lymphocyte ratio (NLR), platelet-to-lymphocyte ratio (PLR), prognostic nutritional index (PNI), and systemic immune-inflammation index (SII), all previously linked to treatment efficacy. Ordered logistic regression analyses identified ultrasound-based basal width reduction rate ($p=0.001$), CT-based lymph node short-axis reduction rate ($p=0.000$), and CT-based tumor thickness reduction rate ($p=0.024$) as key predictors (Table 4). These variables formed the regression model (Supplementary Table 1). Nomograms for the three indicators were constructed (Fig. 2) and validated via ROC curves: AUC = 0.952

Clinical characteristics	Counts (%)
Overall	75 (100%)
Gender	
Male	56 (74.6)
Female	19 (25.4)
Location of primary tumor	
Proximal stomach	26 (34.7)
Body of stomach	18 (24.0)
Distal stomach	31 (41.3)
Case type	
Large Borrmann III type	47 (63.7)
Borrmann IV type	10 (13.3)
Bulky N+	18 (24.0)
Lauren classification	
Intestinal type	26 (34.7)
Diffuse type	40 (53.3)
Mixed type	9 (12.0)
Differentiation	
Moderately differentiated	18 (24.0)
Poorly differentiated	43 (57.3)
Signet ring cell/Mucinous adenocarcinoma	14 (18.7)
cT stage	
4a	75 (100.0)
cN stage	
N+	75 (100.0)
TRG grading	
0 (ypCR)	14 (18.7)
1	23 (30.7)
2	26 (34.6)
3	12 (16.0)
MSI status	
MSS	74 (98.7)
MS-H	1 (1.3)
CPS value	
<1	25 (33.3)
≥1,<5	26 (34.7)
≥5	24 (32.0)
Max. Pre-treatment Lymph Node Short Axis (cm)	
<1.0	21 (28.0)
≥1.0,<1.5	31 (41.3)
≥1.5	23 (30.7)

Table 1. Participants' clinical characteristics.

for TRG_0–1 + TRG_2 vs. TRG_3, AUC = 0.870 for TRG_0–1 vs. TRG_2 + TRG_3, AUC = 0.900 for TRG_3 identification (Fig. 3a, b). Calibration curves confirmed strong alignment between predicted and actual outcomes. DCA curves demonstrated clinical utility (Fig. 3c, d). Given the small sample size, 10-fold cross-validation (70% training, 30% testing) yielded multinomial logistic regression accuracy = 0.73, Dxy = 0.725, and R^2 = 0.757 (Supplementary Table 2). Model applications are summarized in Table 5.

Discussion

In Western nations, perioperative chemotherapy is now the standard for LAGC, supported by trials like MAGIC[27] FNCLCC/FFCD 9703[28], and the FLOT4-AIO study. The NCCN guidelines prioritize this approach, a recommendation shared by Asian scholars through studies like China's RESOLVE and Korea's PRODIGY[29]. PD-1 inhibitors, initially effective in melanoma, have expanded to GC. CheckMate-649[30] demonstrated the first-line efficacy of PD-1 inhibitors + chemotherapy in LAGC, leading to NMPA approval of Opdivo for advanced/metastatic gastric, gastroesophageal junction (GEJ), or esophageal adenocarcinoma. In China, sintilimab (Orient-16, 2022) was approved for unresectable locally advanced/recurrent/metastatic GC or GEJ adenocarcinoma when combined with oxaliplatin + capecitabine. Neoadjuvant immunotherapy + chemotherapy

Metric	RECIST_ Expansion	UC_RECIST	CT_RECIST	V_RECIST	U_RECIST
TRG 0–2 vs. TRG 3					
AUC	0.915	0.909	0.933	0.951	0.906
Std. Error	0.046	0.035	0.038	0.033	0.041
Asymptotic Sig.b	0.000	0.000	0.000	0.000	0.000
Optimal Cutoff value(%)	0.12	0.24	0.12	0.34	0.5
Sensitivity(%)	93.70	76.20	96.80	96.80	88.90
Specificity(%)	77.00	76.20	71.80	80.10	72.20
TRG 0–1 vs. TRG 2–3					
AUC	0.778	0.804	0.842	0.868	0.811
Std. Error	0.053	0.051	0.046	0.042	0.050
Asymptotic Sig.b	0.000	0.000	0.000	0.000	0.000
Optimal Cutoff value(%)	0.31	0.35	0.32	0.61	0.50
Sensitivity(%)	84.20	89.50	89.50	94.70	81.10
Specificity(%)	56.80	62.20	75.70	75.30	68.40

Table 2. ROC curve analysis of neoadjuvant therapy response modelsr: comparing TRG 0–2 vs. TRG 3 and TRG 0–1 vs. TRG 2–3. AUC: Area Under Curve. TRG: Tumor regression grade. RECIST_Expansion: Expanding only the threshold for positive lymph nodes.UC_RECIST: Ultrasound combined with CT assessment, incorporating primary lesion base width.CT_RECIST: CT-only assessment, incorporating primary lesion thickness.V_RECIST: Ultrasound combined with CT assessment, using an approximate volume formula.U_RECIST: Ultrasound-only assessment, incorporating primary lesion thickness and base width.

has shown promise in GC, with studies like Jia et al.[31] and Lin et al.[18] reporting improved response rates and outcomes in locally advanced GEJ adenocarcinoma.

However, evaluating neoadjuvant treatment efficacy in LAGC remains highly Limited. The current RECIST 1.1 criteria classify the primary gastric lesion as a hollow organ, excluding it from measurable targets. Furthermore, metastatic lymph nodes must have a short-axis diameter ≥ 1.5 cm to be considered measurable, which significantly restricts the accuracy and applicability of response assessment. In our study, 69.3% of patients had lymph nodes < 1.5 cm before treatment, leaving many without measurable lesions and thus no basis for standardized evaluation. Additionally, this leads to the exclusion of advanced patients from trials, denying them access to potentially life-saving investigational therapies.

Emerging approaches have been explored for efficacy evaluation in GC, For instance: Yan et al.[32] found contrast-enhanced ultrasound predicted chemotherapeutic responses with 81.8% sensitivity and 66.7% specificity. Wang et al.[33] demonstrated CT-based texture models outperformed subjective imaging features (97.3% vs. 56.0% accuracy). Yuan et al.[34] reported DCE-MRI and IVIM-DWI parameters achieved an AUC of 0.92, with 87.0% sensitivity and 85.0% specificity. Wang[35] combined radiomics/deep learning with PD-L1 expression, improving AUC by 4–7%.Zurlo IV et al.[36] highlighted histological subtype impacts, while Liu C. et al.[37] developed a recurrence-based prognostic model. Alternative criteria Like irRECIST, imRECIST, EORTC, and PERCIST 1.0 have been proposed to better assess immunotherapy outcomes and prognosis. However, none have replaced RECIST 1.1 as the standard.

Gastric cancer's primary tumor is often flat-cylindrical, We observed that treatment-sensitive features detectable by ultrasound at millimeter precision (e.g.basal width and lesion thickness changes). Based on this, we evaluated whether ultrasound-integrated assessments could enhance or replace RECIST 1.1. If validated, this approach could expand RECIST 1.1's applicability, benefiting more patients. We designed two models using high-resolution CT and color Doppler ultrasound: Modified RECIST Framework: RECIST_Expansion: Lymph node assessment only. UC_RECIST: CT-ultrasound integration (gastric lesions as measurable targets). CT_RECIST: CT-only (for facilities without ultrasound). U_RECIST: Ultrasound-only (enables frequent monitoring). V_RECIST: Multimodal volume modeling (geometric approximation). Visualized Nomogram: Built via ordinal regression, offering graphical, individualized predictions of nonlinear outcomes.

The RECIST_Expansion group demonstrated that lowering the lymph node short-axis threshold to 0.7 cm (vs. RECIST 1.1's ≥ 1.5 cm) enabled accurate differentiation between effective/ineffective chemotherapy and MPR/non-MPR groups (AUC: 0.915 and 0.778). Calibration and decision curve analyses confirmed this adjustment maintains high accuracy. However, due to imaging variability, centers should adapt thresholds based on technical capabilities and validation data. The UC_RECIST group explored gastric lesions as measurable targets by combining ultrasound-derived basal width (longest diameter) with CT-based lymph node short-axis changes. It achieved AUCs of 0.909 and 0.804, validating gastric lesions' feasibility as targets. For CT_RECIST, designed for ultrasound-limited centers, CT-only metrics (e.g., maximum lesion thickness) yielded AUCs of 0.933 and 0.842, showing strong diagnostic potential despite CT's cost and radiation exposure limitations.The V_RECIST group integrated ultrasound and CT data to develop an approximate volumetric calculation formula aiming to improve accuracy. It chieving the highest AUC (0.951 and 0.868) among tested models.The U_RECIST group used ultrasound-only metrics for gastric lesion assessment. Compared to CT's high cost and radiation exposure, ultrasound offers a low-cost, radiation-free alternative suitable for frequent monitoring in precision

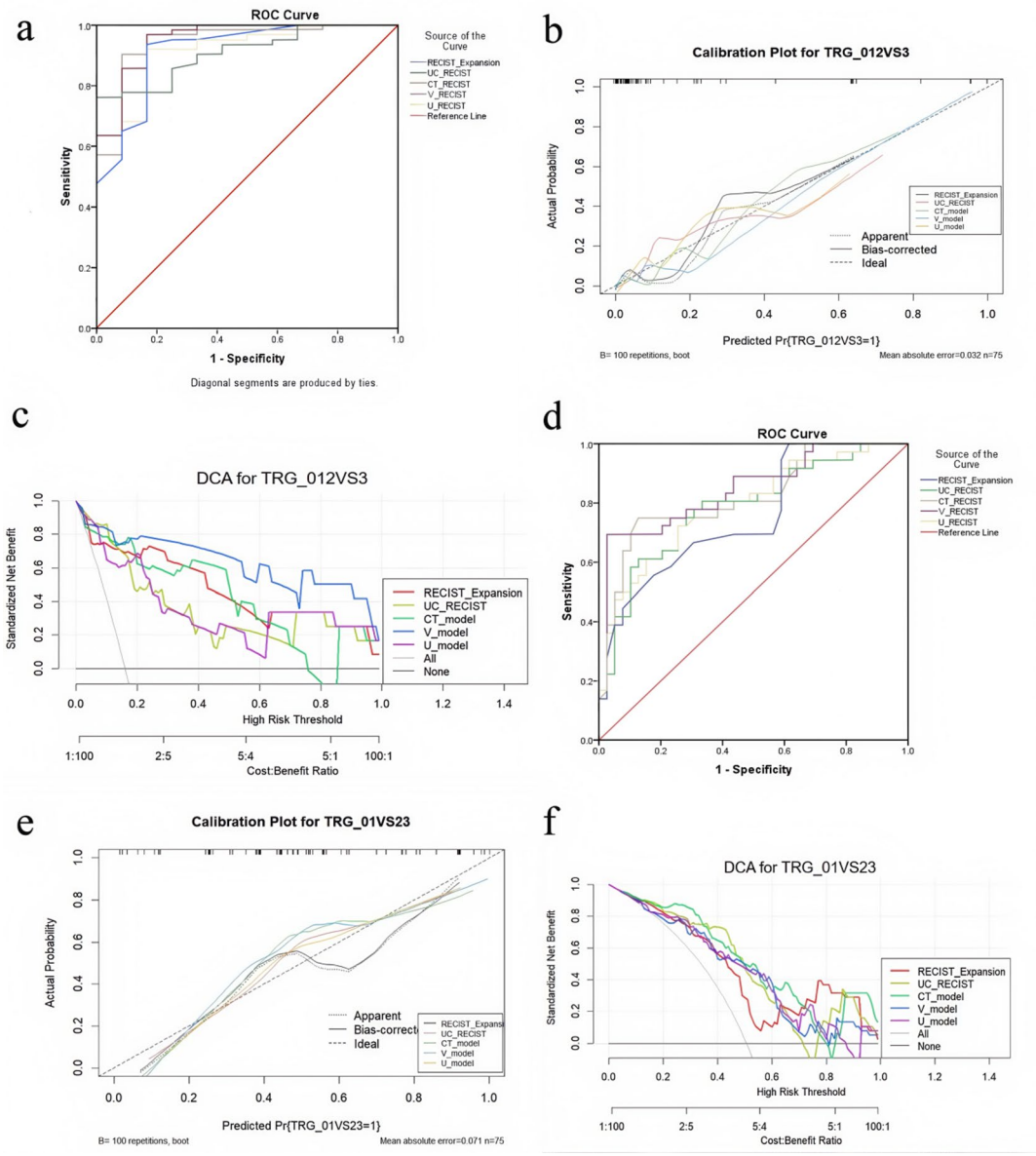

Fig. 1. (**a**) ROC Curve Comparing the (TRG 0–2) and the (TRG 3). (b) Calibration Curves Comparing the (TRG 0–2) and the (TRG 3). (**c**) DCA Curves Comparing the (TRG 0–2) and the (TRG 3). (**d**) ROC Curve Comparing the (TRG 0–1) and the (TRG 2–3). (e) Calibration Curves Comparing the (TRG 0–1) and the (TRG 2–3). (**f**) DCA Curves Comparing the (TRG 0–1) and the (TRG 2–3).

Metric	RECIST_ Expansion	UC_RECIST	CT_RECIST	V_RECIST	U_RECIST
TRG 0–2 vs. TRG 3					
Mean absolute error	0.032	0.037	0.026	0.019	0.053
Mean squared error	0.00192	0.00272	0.00175	0.00099	0.00433
0.9 Quantile of absolute error	0.051	0.087	0.072	0.039	0.115
TRG 0–1 vs. TRG 2–3					
Mean absolute error	0.071	0.028	0.086	0.075	0.039
Mean squared error	0.00635	0.00142	0.00986	0.00769	0.00231
0.9 Quantile of absolute error	0.105	0.066	0.158	0.133	0.090

Table 3. Calibration curve data of neoadjuvant therapy response modelsr: comparing TRG 0–2 vs. TRG 3 and TRG 0–1 vs. TRG 2–3.

Univariate				Multivariate		
Influence Factor	β (95% CI)	*P* Value	OR (95% CI)	β (95% CI)	*P* Value	OR (95% CI)
CPS	0.043 (−0.02, 0.106)	0.181	1.044 (0.980,1.112)			
SⅡ	0.000 (−0.001,0.001)	0.707	1.000 (0.999, 1.001)			
PNI	−0.008 (−0.033,0.018)	0.553	0.992 (0.968,1.018)			
PLR	−0.001 (−0.006,0.004)	0.653	0.999 (0.994,1.004)			
NLR	−0.158 (−0.568,0.252)	0.450	0.854 (0.567,1.287)			
Differentiation	0.577 (−0.101, 1.256)	0.095	1.781 (0.904,3.512)			
USBWR rate	−7.189 (−10.706, 3.672)	< 0.001*	0.001 (< 0.001,0.025)	−8.025 (−12.939, 3.110)	0.001*	0.0003 (< 0.001, 0.045)
CT-LNSAR rate	−10.394 (−14.577, −6.211)	< 0.001*	< 0.001 (< 0.001,0.002)	−9.605 (−14.280, 4.931)	< 0.001*	0.0001 (< 0.001, 0.007)
CT-TTR rate	−7.743 (−11.247, −4.238)	< 0.001*	< 0.001(< 0.001, 0.014)	−4.574 (−8.559, −0.589)	0.024*	0.0103 (0.0002, 0.555)

Table 4. Univariate and multivariate analysis of ordered logistic regression. Statistical Details: Test Method: Ordinal logistic regression, Justification: Appropriate for ordinal outcome variables with continuous/categorical predictors,αLevel:0.05 (two-sided); Proportional Odds Assumption: Met (Brant test, $p = 0.32$);Sample Size: Total $n = 75$ (TRG 0–1: 37,TRG2: 26, TRG3: 12);Reference Category: Highest ordered category (TRG3);P Value Notation: * indicates statistical significance ($p < 0.05$). OR: Odds Ratio. CI: Confidence Interval. CPS: Combined Positive Score.SⅡ: Systemic Immune-Inflammation Index. PNI: Prognostic Nutritional Index. PLR: Platelet-to-Lymphocyte Ratio. NLR: Neutrophil-to-Lymphocyte Ratio. CI: Confidence Interval. USBWR: Ultrasonography-based Basal Width Reduction Rate. CT-LNSAR: CT-based lymph node short-axis reduction rate. CT-TTR: CT-based tumor thickness reduction rate.

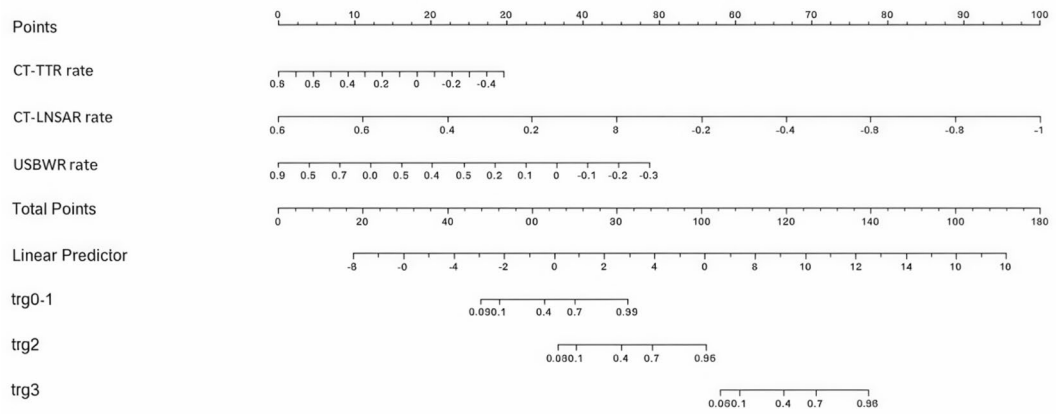

Fig. 2. Nomogram for predicting TRG.

medicine, enabling early detection and personalized treatment. It achieved AUCs of 0.906 and 0.811, slightly lower than V_RECIST but still highly accurate. U_RECIST focused exclusively on primary lesion changes (not lymph nodes). Given that almost all advanced gastric lesions can be measured by ultrasound, this approach has broad applicability, enabling a large number of lymph node-negative GC patients to receive efficacy evaluations and benefit accordingly.

The second model category includes ordinal logistic regression and nomograms, offering visual representation of nonlinear statistical predictions. Patients were classified into three TRG-based groups: MPR (TRG 0–1), partial response (TRG 2), and no response (TRG 3). Univariate analysis incorporated systemic inflammation and nutritional indicators: SII[38] PNI[39] pre-treatment PLR, and NLR[40–42]. Despite prior links to tumor progression, these metrics showed no correlation with pathological tumor reduction—a discrepancy likely due to tumor shrinkage's non-exclusive role in prognosis[43]. While SII/PNI/PLR/NLR may influence prognosis, their impact on neoadjuvant therapy response remains unclear and requires large-scale validation. Combined Positive Score (CPS) quantifies PD-L1 expression via the ratio of PD-L1-positive cells (tumor, lymphocytes, macrophages) to viable tumor cells. Higher CPS is linked to better immunotherapy outcomes[44] yet

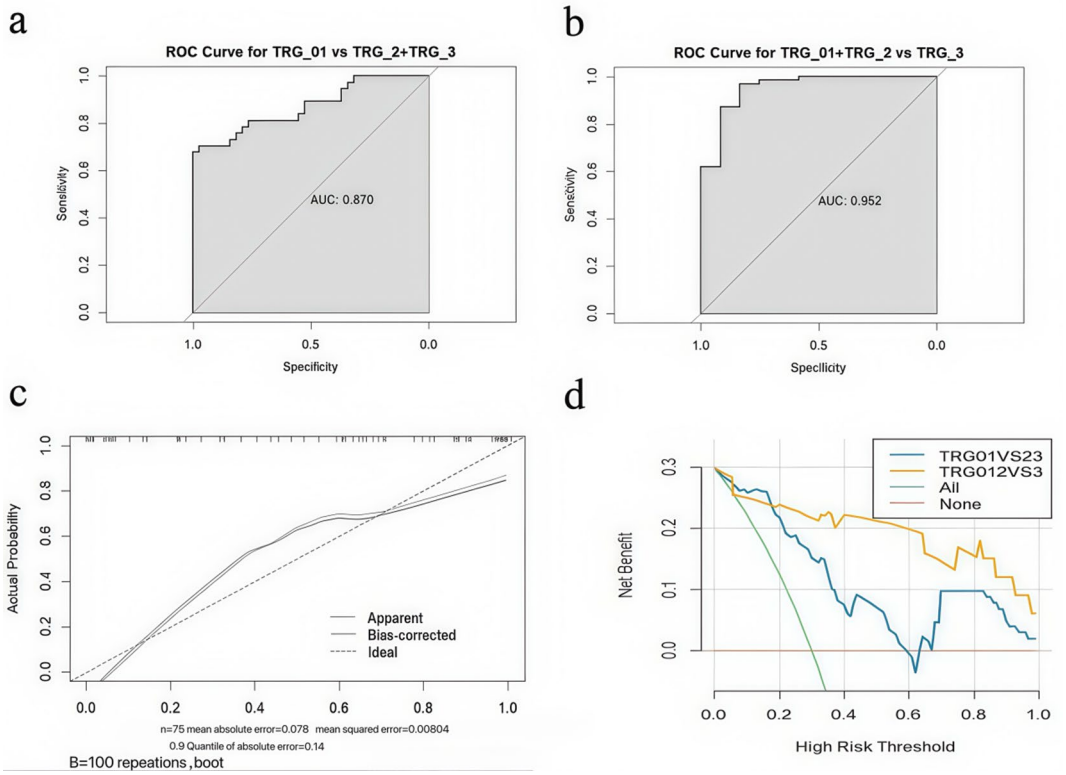

Fig. 3. (**a**, **b**) ROC curves for the nomogram predicting TRG. (**c**) Calibration curve for the nomogram. (**d**) DCA curve for the nomogram.

Model	AUC: TRG 0–2 vs. TRG 3	AUC: TRG 0–1 vs. TRG 2–3	Applicable Scenarios
RECIST_Expansion	0.915	0.778	RECIST 1.1 protocol (lymph node evaluation only)
UC_RECIST	0.909	0.804	CT-US Combined Protocol (gastric lesions as measurable targets)
CT_RECIST	0.933	0.842	CT-Only Protocol (for no-US institutions)
V_RECIST	0.951	0.868	Multimodal Volume Integration (geometric approximation)
U_RECIST	0.906	0.811	US-Only Protocol (enables high-frequency assessments)
Nomogram	0.952	0.870	Ordinal regression nomogram: Predictive visualization tool

Table 5. Application scenarios of different Models. US: Ultrasound, TRG: Tumor Regression Grade, RECIST: Response Evaluation Criteria in Solid Tumors, CT: Computed Tomography, AUC: Area Under the Curve.

no strong CPS-TRG correlation was observed, possibly due to chemotherapy/targeted therapy combinations diluting immunotherapy's individual effect. Three key predictors emerged: Ultrasound-measured basal width reduction ($p = 0.001$) CT lymph node short-axis reduction ($p = 0.000$) CT tumor thickness reduction ($r = 0.024$) A nomogram integrating these factors demonstrated superior predictive accuracy and visual clarity compared to RECIST's linear percentage method. Nomograms, although involving more sophisticated statistical modeling and calculation procedures, demonstrate improved predictive accuracy and visualization. We anticipate that the accumulation of additional clinical data will enable further refinement of the model's performance, thereby facilitating its broader adoption in clinical settings.

Conclusion

Our study comprises six models across two categories. Among these, five RECIST 1.1 modified models exhibit strong performance in evaluating neoadjuvant therapy responses in LAGC patients. The V_RECIST model demonstrates the highest predictive accuracy, while the ultrasound-only U_RECIST model offers cost-effectiveness, radiation-free imaging, and clinically acceptable accuracy, positioning it as a viable option for clinical adoption. The nomogram further improves predictive capacity through advanced statistical modeling and visual clarity. However, real-world validation and model refinement are essential for clinical implementation.

Data availability

The data that support the findings of this study are not publicly available because the primary research is still ongoing. However, they are available from the corresponding author upon reasonable request. The data are stored in a controlled access data repository at Fujian Cancer Hospital.

Received: 30 January 2025; Accepted: 4 September 2025
Published online: 07 October 2025

References

1. Drnovsek, J., Homan, M., Zidar, N. & Smid, L. M. Pathogenesis and potential reversibility of intestinal metaplasia - a milestone in gastric carcinogenesis. *Radiol. Oncol.* **58**, 186–195. https://doi.org/10.2478/raon-2024-0028 (2024).
2. Crimi, F. et al. Predictors of metastatic lymph nodes at preoperative staging CT in gastric adenocarcinoma. *Tomography* **8**, 1196–1207. https://doi.org/10.3390/tomography8030098 (2022).
3. Li, H. et al. Survival of gastric cancer in China from 2000 to 2022: A nationwide systematic review of hospital-based studies. *J. Glob Health*. **12**, 11014. https://doi.org/10.7189/jogh.12.11014 (2022).
4. Zhang, C. et al. Laparoscopic versus open gastrectomy for locally advanced gastric cancer after neoadjuvant chemotherapy: a comprehensive contrastive analysis with propensity score matching. *World J. Surg. Oncol.* **21**, 350. https://doi.org/10.1186/s12957-023-03221-4 (2023).
5. Al-Batran, S. E. et al. Perioperative chemotherapy with fluorouracil plus leucovorin, oxaliplatin, and docetaxel versus fluorouracil or capecitabine plus cisplatin and epirubicin for locally advanced, resectable gastric or gastro-oesophageal junction adenocarcinoma (FLOT4): a randomised, phase 2/3 trial. *Lancet* **393**, 1948–1957. https://doi.org/10.1016/S0140-6736(18)32557-1 (2019).
6. Lin, W., Huang, Z., Du, Z., Wang, Y. & Zuo, T. Case report: clinical application of continuous arterial infusion chemotherapy in neoadjuvant therapy for locally advanced gastric cancer. *Front. Oncol.* **13**, 1214599. https://doi.org/10.3389/fonc.2023.1214599 (2023).
7. Liu, B. W., Shang, Q. X., Yang, Y. S. & Chen, L. Q. Efficacy and safety of PD-1/PD-L1 inhibitor combined with chemotherapy versus chemotherapy alone in the treatment of advanced gastric or gastroesophageal junction adenocarcinoma: a systematic review and meta-analysis. *Front. Oncol.* **13**, 1077675. https://doi.org/10.3389/fonc.2023.1077675 (2023).
8. Miller, A. B., Hoogstraten, B., Staquet, M. & Winkler, A. Reporting results of cancer treatment. *Cancer* **47**, 207-14(1981).
9. Eisenhauer, E. A. et al. New response evaluation criteria in solid tumours: revised RECIST guideline (version 1.1). *Eur. J. Cancer*. **45**, 0–247 (2009).
10. Chun, J. W. et al. Non-sentinel node metastasis prediction during surgery in breast cancer patients with one to three positive Sentinel node(s) following neoadjuvant chemotherapy. *Scientific Reports* **13**, 4480 (2023).
11. Yu, Q., Zhang, H. & Song, J. S. Junkang. Dissociated response to PD-1 inhibitors combined with radiotherapy in patients with advanced metastatic solid tumors: a single-center experience. *World J. Surg. Oncology* **21,** 228 (2023).
12. Shankar, L. et al. Harnessing imaging tools to guide immunotherapy trials: summary from the National cancer Institute cancer imaging steering committee workshop. *Lancet Oncol.* **24** (3), e133–e143 (2023).
13. Yin, K. L. et al. The combination of a prolonged treatment time window and alpha-fetoprotein benefits the tumor response of hepatocellular carcinoma patients as evaluated by the imrecist: a single-center, retrospective study. *J. Gastrointest. Oncol.* **14**, 11 (2023).
14. Park, S., Lee, Y., Kim, T. S., Kim, S. K. & Han, J. Y. Response evaluation after immunotherapy in NSCLC: early response assessment using FDG PET/CT. *Medicine* **99**, e23815 (2020).
15. Annovazzi, A. et al. Prognostic value of [18F]-FDG PET/CT in patients with meta-static breast cancer treated with cyclin-dependent inhibitors. *Front. Oncol.* **13**, 1193174. https://doi.org/10.3389/fonc.2023.1193174 (2023).
16. Stewart et al. Protocol for the examination of specimens from patients with primary carcinomas of the colon and rectum. *Archives Pathol. & Lab. Medicine***133**, 1359-1360 (2009).
17. Frederico, S. C. et al. Neoadjuvant immune checkpoint Inhibition in the management of glioblastoma: exploring a new frontier. *Frontiers Immunology* **14**, 1057567 (2023).
18. Lin, J. X. et al. Neoadjuvant camrelizumab and apatinib combined with chemotherapy versus chemotherapy alone for locally advanced gastric cancer: a multicenter randomized phase 2 trial. *Nat. Commun.* **15**, 12 (2024).
19. Li, N. et al. Efficacy and safety of neoadjuvant sintilimab in combination with FLOT chemotherapy in patients with HER2-negative locally advanced gastric or gastroesophageal junction adenocarcinoma: an investigator-initiated, single-arm, open-label, phase II study. *Int. J. Surg.* **110**, 14 (2024).
20. Saito, T. et al. Accuracy of multidetector-row CT in diagnosing lymph node metastasis in patients with gastric cancer. *Eur. Radiol.* **25**, 368–374 (2015).
21. Cui, Y. et al. A CT-based deep learning radiomics nomogram for predicting the response to neoadjuvant chemotherapy in patients with locally advanced gastric cancer: A multicenter cohort study. *EClinicalMedicine* **46**, 101348. https://doi.org/10.1016/j.eclinm.2022.101348 (2022).
22. Zhou, Z., He, J., Liu, S., Guan, W. & Zhou, Z. [Diagnostic value of magnetic resonance diffusion weighted imaging for metastatic lymph nodes in patients with gastric cancer]. *Zhonghua Wei Chang. Wai Ke Za zhi = Chin. J. Gastrointest. Surg.* **17**, 225 (2014).
23. Bai, H. et al. Predictive values of multidetector-row computed tomography combined with serum tumor biomarkers in preoperative lymph node metastasis of gastric cancer. 中国癌症研究: 英文版. **31**, 10 (2019).
24. Chai, Y. et al. [Preoperative assessment value of spectral CT quantitative parameters in lymph node metastasis of gastric cancer]. *Zhonghua Wei Chang. Wai Ke Za zhi = Chin. J. Gastrointest. Surg.* **20**, 309 (2017).
25. Saddiq, A. A. et al. Antigenotoxicity, and characterization of Calotropis procera and its Rhizosphere-Inhabiting actinobacteria: in vitro and in vivo studies. *Molecules* **27**, 3123 (2022).
26. Hebert, A. H. & Hill, A. L. Impact of opioid overdoses on US life expectancy and years of life lost, by demographic group and stimulant co-involvement: a mortality data analysis from 2019 to 2022. *Lancet Reg. Health Am.* **36**, 100813. https://doi.org/10.1016/j.lana.2024.100813 (2024).
27. Koerner, A. S., Moy, R. H., Ryeom, S. W. & Yoon, S. S. The present and future of neoadjuvant and adjuvant therapy for locally advanced gastric cancer. *Cancers* **15**, 4114 (2023).
28. Wang, X. Z. et al. Interpretation of the development of neoadjuvant therapy for gastric cancer based on the vicissitudes of the NCCN guidelines. 世界胃肠肿瘤学杂志: 英文版(电子版). **12**, 37–53 (2020).
29. Kang, Y. K., Yook, J. H., Park, Y. K., Lee, J. S. & Noh, S. H. PRODIGY: A phase III study of neoadjuvant docetaxel, oxaliplatin, and S-1 plus surgery and adjuvant S-1 versus surgery and adjuvant S-1 for resectable advanced gastric cancer. *Journal Clin. Oncology* **39**, 2903-2913 (2021).
30. Cao, X. et al. First-line nivolumab plus chemotherapy versus chemotherapy alone for advanced gastric cancer, gastroesophageal junction cancer, and esophageal adenocarcinoma: a cost-effectiveness analysis. *Therapeutic Adv. Med. Oncology* **15**, 17588359231171038 (2023).
31. Wei, J. et al. Neoadjuvant sintilimab in combination with concurrent chemoradiotherapy for locally advanced gastric or gastroesophageal junction adenocarcinoma: a single-arm phase 2 trial. *Nature Communications* **14**, 4904 (2023).

32. Yan, C. X. et al. Value of double contrast-enhanced ultrasound QontraXt three-dimensional pseudocolor quantitative analysis to therapeutic effect evaluation of preoperative neoadjuvant chemotherapy in advanced gastric cancer patients. *Zhonghua Zhong Liu Za Zhi [Chinese J. Oncology]*. **40**, 857–863 (2018).
33. Wang, Y. K. et al. Accuracy comparision of abdominal enhanced CT and endoscopic ultrasound in the staging of gastric cancer after neoadjuvant chemotherapy: a post hoc analysis of a randomized clinical trial]. *Zhonghua Wai Ke Za Zhi*. **58**, 614–618. https://doi.org/10.3760/cma.j.cn112139-20200114-00027 (2020).
34. Yuan, Q. et al. Quantitative diffusion-weighted imaging and dynamic contrast-enhanced characterization of the index lesion with multiparametric MRI in prostate cancer patients. *J. Magn. Reson. Imaging*. **45**, 908–916. https://doi.org/10.1002/jmri.25391 (2017).
35. Wang, X. et al. Cancer immunotherapy response prediction from multi-modal clinical and image data using semi-supervised deep learning. *Radiother Oncol.* **186**, 109793. https://doi.org/10.1016/j.radonc.2023.109793 (2023).
36. Zurlo, I. V. et al. Treatment of Locally Advanced Gastric Cancer (LAGC): Back to Lauren's Classification in Pan-Cancer Analysis Era? *Cancers (Basel)*. **12** https://doi.org/10.3390/cancers12071749 (2020).
37. Liu, C., Lu, J. & An, L. Development and validation of nomograms for predicting the prognosis of early and late recurrence of advanced gastric cancer after radical surgery based on post-recurrence survival. *Med. (Baltim).* **103**, e38376. https://doi.org/10.1097/md.0000000000038376 (2024).
38. Jomrich, G. et al. High systemic Immune-Inflammation index is an adverse prognostic factor for patients with gastroesophageal adenocarcinoma. *Ann. Surg.* **273**, 532–541. https://doi.org/10.1097/sla.0000000000003370 (2021).
39. Xiao, Y. et al. Association among prognostic nutritional index, post-operative infection and prognosis of stage II/III gastric cancer patients following radical gastrectomy. *Eur. J. Clin. Nutr.* **76**, 1449–1456. https://doi.org/10.1038/s41430-022-01120-7 (2022).
40. Karra, S. et al. Diagnostic utility of NLR, PLR and MLR in early diagnosis of gastric cancer: an analytical Cross-Sectional study. *J. Gastrointest. Cancer*. **54**, 1322–1330. https://doi.org/10.1007/s12029-023-00937-0 (2023).
41. Zurlo, I. V. et al. Predictive value of NLR, TILs (CD4+/CD8+) and PD-L1 expression for prognosis and response to preoperative chemotherapy in gastric cancer. *Cancer Immunol. Immunother*. **71**, 45–55. https://doi.org/10.1007/s00262-021-02960-1 (2022).
42. Liu, C., Tao, F., Lu, J., Park, S. & An, L. Defining nomograms for predicting prognosis of early and late recurrence in gastric cancer patients after radical gastrectomy. *Med. (Baltim).* **102**, e35585. https://doi.org/10.1097/md.0000000000035585 (2023).
43. Vecchio, F. M. et al. The relationship of pathologic tumor regression grade (TRG) and outcomes after preoperative therapy in rectal cancer. *Int. J. Radiat. Oncol. Biol. Phys.* **62**, 752–760. https://doi.org/10.1016/j.ijrobp.2004.11.017 (2005).
44. Fan, L. et al. First-line treatment options for advanced gastric/gastroesophageal junction cancer patients with PD-L1-positive: a systematic review and meta-analysis. *Ann. Med. Surg. (Lond)*. **85**, 2875–2883. https://doi.org/10.1097/ms9.0000000000000765 (2023).

Acknowledgements

This work was financially supported by the Natural Science Foundation of Fujian province (2022J011060),IIT Funds of Fujian Cancer Hospital.(Grant number:202413002), and the High-level Talent Training Program of Fujian Cancer Hospital (2024YNG08).

Author contributions

LC designed the research. JJ, SL and XC performed and analyzed the study and wrote the paper. ZY and JC provided study materials of patients. CW, YW and YZ participated in the collection and assembly of data, XW analyzed and interpreted the data. SC wrote the first draft of the manuscript. SC and SW contributed to the manuscript refinement. All authors read and approved the final manuscript.

Declarations

Competing interests

The authors declare no competing interests.

Ethical approval

This study was conducted in accordance with the Declaration of Helsinki and authorized by the Fujian Cancer Hospital ethics committee (Ethical approval number: K2023-066-01; ChiECRCT20210434). Before participating in the trial, all patients signed informed consent documents.

Additional information

Supplementary Information The online version contains supplementary material available at https://doi.org/10.1038/s41598-025-18988-7.

Correspondence and requests for materials should be addressed to L.C.